*Korean J. Chem. Eng.*, 32(3), 486-493 (2015)
DOI: 10.1007/s11814-014-0226-9

pISSN: 0256-1115
eISSN: 1975-7220

# A conical shape-evolution model for the control of sapphire crystal growth in Kyropoulos (KY) method

**Do Won Song*,**, Kwang Seok Kim***, and Hyo Kim*,†**

*Department of Chemical Engineering, The University of Seoul, 163, Siripdae-ro, Dongdaemun-gu, Seoul 130-743, Korea
**Siltron Inc., 164-2, Simi-dong, Gumi, Gyeongbuk 730-724, Korea
***Institute of Gas Safety R&D, Korea Gas Safety Corporation,
1390, Wonjung-ro, Eumseong-gun, Chungbuk 369-811, Korea
(*Received 27 February 2014 • accepted 5 August 2014*)

**Abstract**−Generally, the process of sapphire crystal growing in the KY furnace has to be monitored in order to reduce the power of heater continuously as the crystal grows to occupy the crucible. However, it has been difficult to control the heater power as the weight and diameter of crystal change because the solid-liquid interface could not be easily located from on-site measurement. Hence, first, the model was developed to locate the crystal-melt interface and to estimate its dynamic feature during the crystal growth by incorporating the mass and the force balances. This model was applied to analyze the data obtained from the industry-scale crystal growth experiment (for the production of the sapphire crystals in the KY method). Finally, the shape and the dynamic feature of crystallizing front are analytically verified by generating some bands of small bubbles along the crystal-melt interface called a comb-pattern experiment.

Keywords: Conical Shape-evolution Model, Sapphire Crystal, Kyropoulos Method, Mass and Force Balances, Comb-pattern Experiment

## INTRODUCTION

Recently, there has been an upsurging industrial interest in employing sapphire crystal as a substrate for high-brightness LED and as an active luminescent crystal device. Since the physical and chemical characteristics of single-crystal sapphire ($Al_2O_3$) including thermal stability and mechanical strength are most suitable to such applications, it is expected the demand of sapphire substrates will increase as ICT and digital display markets expand exponentially in the next decade [1].

In the industry, due to the high productivity and relatively low cost, two methods are usually emplemented to grow sapphire crystal: the KY method and the heat exchange method (HEM). Although both are based on the recovery of the latent heat from the melt, the KY method is known more advantageous in terms of the direct automatic control of the crystal growth (i.e., controllability), the product quality and the cost effectiveness, compared to the HEM. First, during the KY process, crystal-pulling force is measured at pre-determined time points, which is necessary for the crystal growth control. However, during the HEM process, only temperature can be measured at a position of interest, but crystal-pulling force can not. Temperature itself does not provide sufficient information for the control. Note that, during the Czochralski (CZ) process, crystal diameter can be measured, which can be alternatively used for the crystal growth control. Second, Vishnevskii et al. have reported that, during the HEM process in a carbon-containing medium, the deviation from the melt stoichiometry causes excessive aluminum ions, and the coagulation of vacancies and the excess aluminum ions leads to the formation of submicron inclusions at the solid-liquid interface in the course of the phase transition [2,3]. Third, in the course of the HEM process, a great deal of gaseous helium should be consumed as coolant.

In the KY method, as a sapphire crystal grows, the power of heater is reduced gradually and in a controlled way. As a result, the temperatures of melt and crucible are decreased. The control algorithm (for the direct automatic control) is highly dependent on the weight gain of ingot, and thus it should be carefully monitored over the entire process [4]. It is important to address that the precise tracing of the solid-liquid interface is most challenging because the solidification takes place at an extremely low rate, and thus there exist more than one unidentified disturbance (including even an aged heat shield). Once the ingot comes in contact with the crucible, many issues arise: loss of controllability, defects breakout, low angle grain boundary (LAGB) and cracks.

There have been continuous efforts made to overcome the challenges and to build unique control logics. Demina et al. have presented a 2D numerical simulation for the sapphire crystal growth in the KY method. Their approach employs a minimal set of simplifications and estimates the temperature at any point of the furnace to design the heat shield. Their model estimates the temperature gradients in the crystal and melt, the heat flux distribution depending on the materials of the furnace parts, the geometry of the solid-liquid interface and the power consumption [5]. Demina and Kalaev have applied a 3D unsteady melt convection for the crystal-melt interface formation. And they have pointed there is a strong effect of radiative transfer onto the crystal at the solid-liquid interface

†To whom correspondence should be addressed.
E-mail: hkim@uos.ac.kr

and a suitable use of material properties such as viscosity which has to be applied to estimate the velocity of melt flow and the solid-liquid interface shape [6]. Chen et al, have employed a numerical computation to investigate the temperature and velocity distributions in the crystal and melt with a specific crystal shape for the sapphire crystal growth with a given input power history. They have concluded the solid-liquid interface is always convex towards the melt with the convexity increasing as the input power decreases before the crystallization front is close to the bottom of the crucible. Then around the crucible bottom, the convexity of the solid-liquid interface decreases so that the crystal apex becomes flat [7,8].

Xu et al. have developed the SAMPAC (Sapphire growth technique with micro-pulling and shoulder-expanding at cooled center) method based on the heat shield configurations of KY furnace combined with the operational method of CZ technique. In the SAMPAC method, in order to design the temperature field, they have designed their own heater and thermal insulation screen (namely radiator) with a certain structure which will make the lower heater resistance larger than the upper one. The radiator has been adjusted to accomplish the process of crystal necking and shouldering. And they have concluded, by optimizing with a numerical simulation and experimental analysis, that a good quality sapphire can be grown within the ranges of 1.0-5.0 mm/hr of growth rate and 10-30 K/hr of temperature decreasing speed in a-axis growth direction [9]. Zhang et al. have theoretically analyzed the shape evolution of crystal by pulling it in KY and SAMPAC methods to devise the process for the shape controlling. They have applied their shape-evolution model through by integrating the quantity kinematical relation at a 1D crystallization process to find out the affecting parameters on the crystal shape during a practical growth. To get an optimal process during the iso-diameter crystal growth, they have reduced the pulling rate and the heater temperature simultaneously [10,11]. Even though the iso-diameter undergoes successive changes during the crystal growth in the SAMPAC method, they have assumed that the solid-liquid interface as a cone with a fixed apex angle. In a practical crystal growth in the KY furnace, however, it is very hard to get a model relating the crystal diameter changes to the process parameters such as pulling rate, advancing speed of crystallization front and heater temperature without considering the changes of crystal-melt interface.

Thus, a more feasible and applicable method named SK Forecast has been recently developed by the Institute for Single Crystal and Alyuda Research LLC in Ukraine [12]. It is a forecasting and analyzing program for the dynamic growing feature during the KY process by employing an approximated cone-shaped interface. The input parameters for the program are the pulling speed and force of the growing crystal and the diameter measured from as-grown crystal with an initial guessing value of cone angle. The aim of the SK Forecast program is to evaluate if the growing process is kept in a proper track to meet the good quality of sapphire without any defect under a given heat shield configuration. Therefore, for this purpose we have to obtain, with the help of pervious results from the several successful runs of crystal growth, the desirable dynamic parameters such as the changes of apex angle with an assumed cone shape at the crystal-melt interface and crystal diameter including the speed of crystallization front. The obtained profile of pulling weight history can play a role of target to be sought for a new crystal growing process under the same growing conditions. However, the SK Forecast program failed occasionally in its calculation because the time interval taken to measure the pulling force during the crystal growth is so big that the force profile cannot represent a real crystal shape accurately. To avoid this problem we proposed a simplified method by employing direct calculations of crystal mass and force changes with an assumed conical shape-evolution model.

## MODEL FORMULATION

In order to model the crystal growth by the KY method, the closed system is defined: (i) the growing crystal, (ii) the melt that loses its mass as the crystal grows, and (iii) the crystal-melt interface that moves outward. The melt is in constant contact with the crucible or air. Since the temperature is less than the $Al_2O_3$ melting point, i.e., sub-cooled liquid, neither the dissociation nor the evaporation takes place. The rate of decrease in the power of heater is extremely low so that the heat transfer through the melt bulk can be readily ignored and it is assumed that the temperature is in a flat profile (a quasi-steady state). Heat is released as a result of the solidification at the crystal-melt interface and the transfer of the heat plays a key role in determining the speed of crystallization front [13]; however, the latent heat does not influence the temperature profile in the melt bulk because of its extremely slow release. For this reason, the equation for the energy balance is not taken into consideration in this modelling. In the Appendix, this heat transfer problem is addressed in an equation-oriented approach. It is important to note that, in industrial practice, the crystal growth as a result of the heat loss at the crystal-melt interface is monitored through a direct pulling-force measurement.

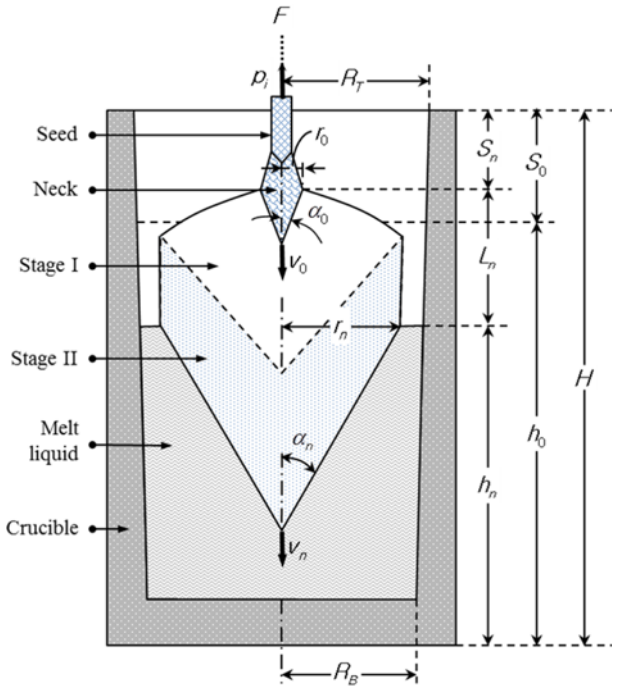


**Fig. 1. The configuration of a conical shape-evolution model for sapphire growing in KY method.**

In our geometric model, as shown in Fig. 1, the growing stages are divided into three stages. The first stage represents the shoulder growing process after the seed crystal has been pulled to make a neck (Stage I). The second stage accounts for the body growing process before the crystal apex touches the crucible bottom (Stage II). The final stage is for the crystal growing up to occupy the remained space followed by Stage II. The growing crystal is slowly pulling up at a programmed speed during the crystallization but the crucible is stationary. During the Stage I and II, the growing system has been considered in two parts of crystal and liquid with an axial symmetry. Since the sapphire mass within the grower is always composed of growing crystal and contracting melt, the total mass during the crystallization is kept as the initially charged mass, and so the following equation for the mass conservation is obtained,

$$M_0 = M_c + M_l. \tag{1}$$

Here the subscripts 0, c and $l$ represent the initial state at Stage I, crystal and liquid, respectively. The growing crystal has a conical shape at the solid-liquid interface as shown in Fig. 1. The mass of crystal is a sum of the floated and submerged parts. As the crystal is growing up and the melt is descending down, the growing crystal mass will be determined by considering the pulling speed $p_i$ and the melt height changes $(h_i - h_{i+1})$ in a time dierence $\Delta t = t_{i+1} - t_i$ for i=0, 1, 2, …, n where n is the number of time intervals up to the time t from $t_0$ (the dierence scheme between i+1 and i is used to account for the discrete measurement system on site). The equation for the crystal mass built up at the crystallization time $t(=n\Delta t)$ is described as

$$M_c = \frac{\pi\rho_c}{3}\left[\sum_{i=0}^{n-1}\left\{\left(\frac{p_{i+1}+p_i}{2}\right)\Delta t + (h_i - h_{i+1})\right\}\Phi(r_{i+1}, r_i) + r_n^3\cot\alpha_n\right]. \tag{2}$$

The subscript n means the value at time t. The mass fragments of growing crystal in every $\Delta t$ have been added to represent the crystal mass grown for time t. Here the programmed pulling speed is applied as an arithmetic average value during $\Delta t$. Applying the proposed conical shape-evolution model, the floated part above the melt surface will look like a pile of truncated cones while the submerged one is maintained in a cone shape.

After taking account of the submerged part of the crystal, the mass of liquid at time t is determined by

$$M_l = \frac{\pi\rho_l}{3}\{h_n\Phi(R_B + \delta h_n, R_B) - r_n^3\cot\alpha_n\}. \tag{3}$$

In the above equations $\rho$, h, r and $\alpha$ are the density, melt height, radius of growing crystal at the melt level and halved apex angle on solid-liquid interface, respectively (Fig. 1). The pulling speed of crystal is given by a programmed recipe while the informations for the melt height, crystal radius and apex angle are not supplied by the on-site measurements. The function $\Phi(A, B) = A^2 + AB + B^2$ is introduced to calculate the volume of cone, truncated cone and cylinder altogether by using the same equation. In Eq. (3) $\delta(>0)$ is a characteristic dimensionless number defined as $(R_T - R_B)/H$ for calculating the crucible radius at the melt level. Here $R_T$, $R_B$ and H are the radii of top and bottom, and height of the crucible, respectively, as shown in Fig. 1.

The crystal pulling force Fn acting on the growing crystal is balanced with the gravitational force $M_c$ g (g is the acceleration of gravity) subtracted by the buoyancy force:

$$F_n = \frac{\pi\rho_c g}{3}\sum_{i=0}^{n-1}\left\{\left(\frac{p_{i+1}+p_i}{2}\right)\Delta t + (h_i - h_{i+1})\right\}\Phi(r_{i+1}, r_i) + \frac{\pi(\rho_c - \rho_l)g}{3} r_n^3\cot\alpha_n. \tag{4}$$

The first term on RHS of Eq. (4) is the weight of the ingot above the liquid level and the second term represents the buoyancy force of the submerged part. The crystal pulling force is the same as the string tension which is attached to a load cell at one end and to the top of the seed shaft at the other end. Since the density of sapphire crystal is greater than that of the melt (the density ratio=0.75 ($\rho_l$=3.03 g/cm$^3$ and $\rho_c$=3.97 g/cm$^3$)), the net weight is downward, and the string is subjected to stretch.

Total number of decision variables in Eq. (1)-Eq. (4) will be four ($h_n$, $r_n$, $\alpha_n$, $M_c$) because the other ones can be obtained from the measuring instruments or from the operating conditions under a given crucible geometry. However, we have three independent equations of Eq. (2), Eq. (3) and Eq. (4). Hence, one more piece of information needs to be provided because of the four unknowns. Usually when a grower is designed for sapphire crystal growth in KY method, there will be several runs of test growing in advance of commercial growing start-up. By examining the successfully grown crystals (so-called boules) in the test runs, the target value of crystal radius $r_n(t)$ will be obtained. Therefore, we can get $r_n(t)$ from the test-run measurement of crystal-radius changes, and the unknowns $h_n$, $\alpha_n$ and $M_c$ can be solved with Eq. (2) (or Eq. (1)), Eq. (3) and Eq. (4). First, to find out $h_n$, applying Eq. (2) and Eq. (3) into Eq. (4) with $M_0 = M_c + M_l$, the equation for $h_n$ is derived

$$h_n\Phi(R_B + \delta h_n, R_B) = \frac{3}{\pi\rho_l}\left(M_0 - \frac{F_n}{g}\right). \tag{5}$$

Eq. (5) is a cubic polynomial for $h_n$ which is solved iteratively by using Newton's method. After obtaining $h_n$, the values of $\alpha_n$ and $M_c$ can be calculated from Eq. (4) and Eq. (2), respectively. Or $M_c$ can be obtained from Eq. (3) by using of $M_c = M_0 - M_l$, too. The discrepancy between $M_c$s from Eq. (2) and Eq. (3) has been adjusted by changing the values of $\alpha_n$. This adjustment of $\alpha_i$ for i=0, 1, 2, …, n throughout all the time t determines the solid-liquid interface evolving in a conical shape before touching the bottom wall. For all over the calculations at every $\Delta t$, the values of $\alpha_i$ are first guessed and then corrected when the following convergence criterion is achieved

$$\|M_c \text{ from Eq. (2)} - M_c \text{ from Eq. (3)}\| < \varepsilon. \tag{6}$$

We have $\varepsilon = 1\times10^{-4}$ used in the later calculation. In addition, the increasing crystal length $L_n$ at time t can be determined as

$$L_n = h_0 - h_n + \sum_{i=0}^{n-1}\left(\frac{p_{i+1}+p_i}{2}\right)\Delta t. \tag{7}$$

Because the crucible height $H = h_n + L_n + S_n = h_0 + S_0$ where $S_n$ is the length from the crystal shoulder to the crucible top at time t and defined as $S_0 - \Sigma_{i=0}^{n-1}(p_{i+1}+p_i) = 2$ (see Fig. 1). When we apply this conical shape-evolution model into the sapphire crystal growth in KY method, the optimal growth rate according to the pulling force could

be characterized in any grower system. Throughout this calculation we can get the apex position profile at the crystal-melt interface with time. That means, not only we know the peak-moving speed as the crystallization proceeds without any other melt flow simulation, but also we can set a criterion to determine whether the crystal will have any defects such as bubbles and LAGB or not, in a given heat shield configuration.

## GROWTH CONTROL METHOD

Under the industrial-scale crystal growth conditions such as high temperature (over 2,030 ℃) and ultra-high vacuum (below $10^{-6}$ Torr), the automatic growth control algorithm for the KY furnace is not yet sufficiently developed, while it is already set up for the CZ equipment [14]. To take the full advantages from the KY equipment, the growth control procedure is proposed in this study as follows: (1) build up the standard regimen for the pulling force as a function of time; (2) during the growth, compute by applying the shape-evolution model and the growth rate $dM_c/dt$ developed in the previous section; (3) increase or decrease the pulling force according to the deviation of from its standard value. For the step (1), several real-scale try-and-error tests are necessary where the pulling force and the radius of the boule throughout each test should be recorded. In the step (3), the time derivative of Eq. (4), $dM_c/dt$, $dr_n/dt$ and $d\alpha_n/dt$ are used. The steps (2) and (3) are repeated with a constant time interval until the crystal growth completes. In the end, the crystal quality is determined. It should be noted that, during the crystal growth, the pulling force and the radius profiles are recorded so that the profiles for the ingot that passes the quality inspection can be used later as another standard regimen.

Generally, as shown in Fig. 2, the whole shape of grown crystal is an irregular lump such as a pear. However, in every Δt it can be assumed a truncated cone. In the SK Forecast, the pulling force is recorded with some time interval while the crystal radius is used with a manually measured one along the a-axis interval from the test-run boule, so the crystal growth predicting program frequently fails due to the mismatch between the data collection time intervals. In order to reduce these failures between the real and assumed crystal shapes or the mismatch between the pulling-force measurement period and radius-calculation time interval, we have employed the conical shape-evolution model proposed in the previous section by applying the same time interval Δt as in both pulling force and radius measurements. The target profile and its operational range are determined by applying the proposed model equa-

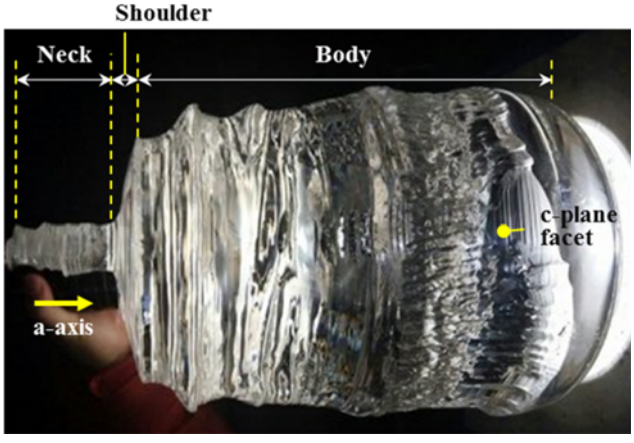


**Fig. 2. A photo of 85 kg sapphire crystal grown by proposed growth control method.**

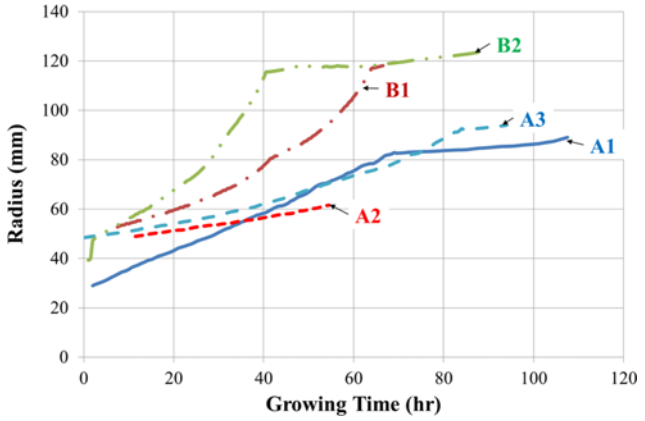


**Fig. 3. The measured radius $r_n(t)$ from several test runs in a 85 kg sapphire grower.**

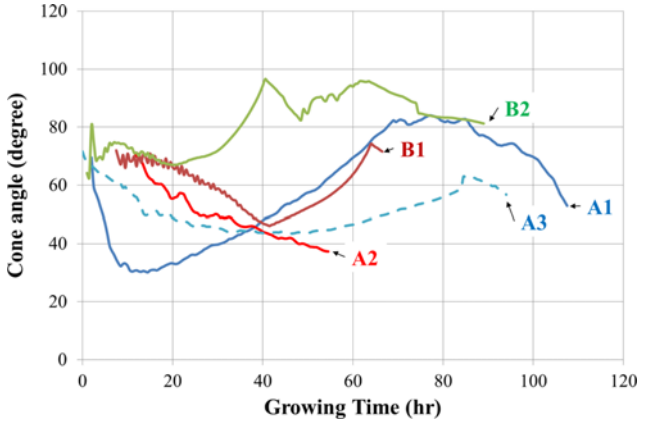


**Fig. 4. The calculated cone angle ($2\alpha_n$) from several test runs in a 85 kg sapphire grower.**

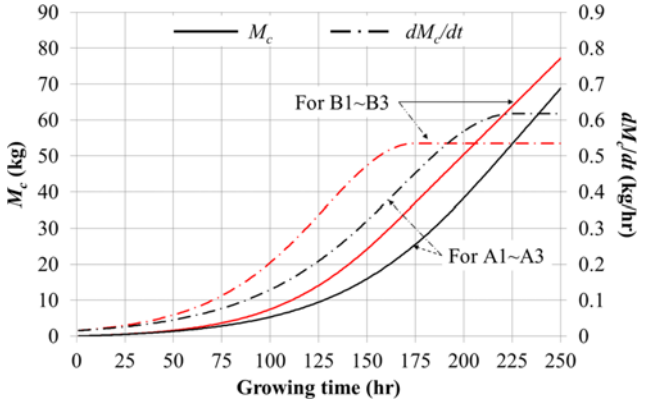


**Fig. 5. The calculated profiles of mass $M_c$ and growth rate $dM_c/dt$ in a 85 kg sapphire grower.**

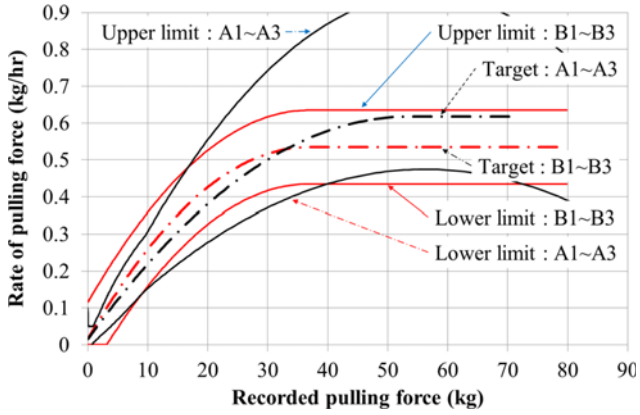


**Fig. 6. Target profile of $dF_n/dt$ and its operational range according to the recorded $F_n$ in the test runs.**

tions as well as by avoiding the undesirable aspects such as LAGB and bubbles in the crystal, and sticking to the crucible wall during the test runs. Fig. 3 and Fig. 4 by employing 5 test runs have shown the measured radius $r_n(t)$ and calculated cone angle $2\alpha_n(t)$, respectively. And Fig. 5 has shown the calculated mass $M_c$ and mass growth rate $dM_c/dt$ which will be used to get a target profile. Finally, in Fig. 6, the adjusted target for the rate of pulling force $dF_n(t)/dt$ and its lower and upper limits for B1-B3 boules are derived from several test runs of a 85 kg sapphire-crystal growing in KY method in the domain of recorded pulling force. Here the test runs are named as A1-A3 and B1-B3 whose operation conditions are explained in the experimental section. In addition, in our conical shape-evolution model, the Stage I and II is divided at a time when the solidification has been finished in 10%.

## EXPERIMENTAL

To confirm how well the proposed growth control model works for the production of a defect-controlled sapphire crystal in the KY method, experimentally several crystal boules in a 85 kg crystal grower are grown under some different operation conditions (see Table 1). The crackle-type sapphire poly-crystal (EMT Inc., Franklin Park, IL) and beads-type alumina (RSA) with 4.5 N purity degree have been used as raw materials. Particularly, the crucible, heater and heat shields have been annealed in a high vacuum state to reduce the pollution caused by oxidization of molybdenum, tungsten, alumina-granule and zirconia bricks.

Using the Insight-1000 equipment (DK AZTEK [15], Korea) with a tungsten crucible and a traditional bird-cage heating element, we have grown six crystals. Three of them are grown under the original heat shield configuration provided by DK AzTEK (A1-A3 boules). And the others (B1-B3 boules) have grown under some modifications of the bottom- and side-shields, in which we have changed the insulation materials from granular-typed alumina to chip-typed molybdenum in both of the bottom and side regions except for the heater and crucible, and the raw materials have been charged lesser by 3 kg than those of A1-A3 boules. The target and control limits of A1-A3 boules have been calculated by using previous several test runs and then we have got the target and control limits of B1-B3 by employing the growth data of A1-A3 boules in our conical shape-evolution model. Through all of the crystal growing the heater power has been controlled to get a desirable growth rate in a given heat shield. In order to control the power of heating elements as the crystallization proceeds we have used a general proportional-integral controller without the derivative logic because the growth rate is very slow in sapphire crystal and the power change is immediately aecting the temperature distribution in the melt by the radiation. Moreover, in order to maintain the growing conditions, we have controlled the growth rate with the slope of heating power rate, which is an eective way to shorten the time lags because of the low growth rate and aging effect under the circumstances of high temperature and low vacuum.

In addition, Bianchi and Viskanta have shown theoretically that the density and size of bubbles within the crystal are affected by the solidification rate in a directional solidification. And they experimentally have shown in the solidification of water that the size and density of generated bubbles are determined by the speed of solidification. At a solidification rate of 36 mm/hr, bubbles nucleate over entire interface and are entrapped by the solid, but at a rate of 3.6 mm/hr, almost no bubble nucleates [16]. Thus, in order to identify the shape and dynamic features of crystal-melt interface in different growth stages with a given heat shield configuration, we could generate some bands of small bubbles intensively along the crystal-melt interface by increasing the speed of crystallization through a suitable power drop in the B3 boule, which is named a comb pattern experiment. When the pulling force of growing crystal reaches a specific value, we have dropped the heater power by about 3-4% from the designed value and then after 25-35 minutes we let the power restore to its original designed level, which has been repeated

**Table 1. Sapphire boules produced by the test runs in a 85 kg grower and their operation conditions**

| Boule | Raw material composition [kg] | | Operating conditions | | | | Crucible dimension [mm] |
|---|---|---|---|---|---|---|---|
| | Crackle | Bead | Initial power [kW] | Total decreased power [kW] | Growing time [hr] | Pulling distance [mm] | |
| A1 | 61 | 24 | 89.64 | 11.09 | 325 | 36.7 | Diameter: 310 Height: 436 |
| A2 | | | 104.08 | 11.82 | 269 | 40.3 | |
| A3 | | | 92.56 | 11.44 | 280 | 36.7 | |
| B1 | 60 | 22 | 97.52 | 12.54 | 248 | 35.9 | |
| B2 | | | 92.81 | 12.09 | 251 | 82.9 | |
| B3 | | | 98.36 | 9.18 | 277 | 34.0 | |

throughout the whole process (see (c) in Fig. 9). During this comb pattern experiment, we controlled the pulling force manually. In addition, in order to evaluate the crystal defects, the grown sapphire crystals have been cut vertically into 3-5 mm thick slugs along the growth direction (a-axis). By placing these slugs under the polarized light, we have examined the existence of crystal defects.

## RESULTS AND DISCUSSION

By applying the proposed conical shape-evolution model at the solid-melt interface in the KY method, the target profile of the rate of pulling force and its operational range are derived by using the measured data of $r_n(t)$ and the calculated data of $\alpha_n(t)$, $M_c(t)$ and $dM_c(t)/dt$ in 5 test runs in a 85 kg sapphire grower. The operational control limits are plotted in the domain of recorded pulling force $F_n$ and the rate of pulling force $dF_n/dt$ for 5 test runs except B3 (A1-A3 and B1-B2 boules are in Fig. 7 and Fig. 8, respectively). Here A1-A3 boules grown under the same grower are of ugly cases because of the generated LAGB in the neck stage or prematured touch to the crucible bottom during Stage I (see Fig. 3 and Fig. 4). Conclusively, two test runs of B1 and B2 are successful and the others are failed as we can expect from Fig. 7 and Fig. 8. From the results shown in Fig. 7 the test runs of A1-A3 display very broad and unbounded spectrum in the rate of pulling force, which is ominous of the growing crystal quality. Therefore, it has confirmed that the proposed growth control method can be applied for the production of defect-controlled sapphire in KY method. The shape of crystallization front will be varied to a given heat shield as crystal grows, and its dynamic parameters could be modelled according to our approaching method.

It is possible to anticipate the outbreak of the defects and its type from by studying the graph of the growth rate [g/hr] vs. the pulling force [kg]. By and large, there are 3 representative patterns observed in the graph when one or more defects occur:

(1) a rapid increase of the growth rate over the upper limit for a long time (more than 10 hours) indicates LAGB, i.e., polycrystalline formation the density of which is generally greater than that of single crystalline;

(2) an oscillating pattern between the upper and the lower limits is a precursor to the bubble formation; and

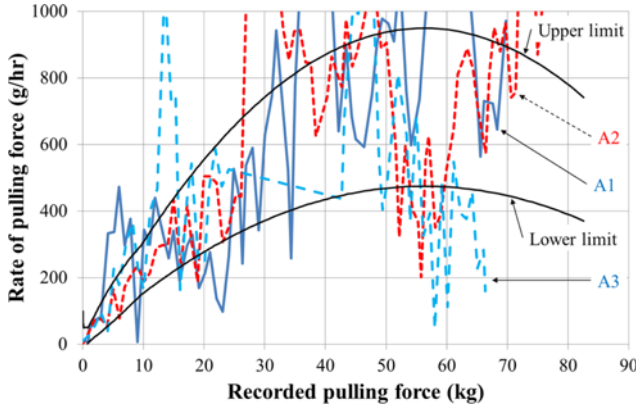


**Fig. 7. The operational control limits of $dF_n/dt$ according to the recorded $F_n$ from A1-A3 test runs in a 85 kg sapphire grower.**

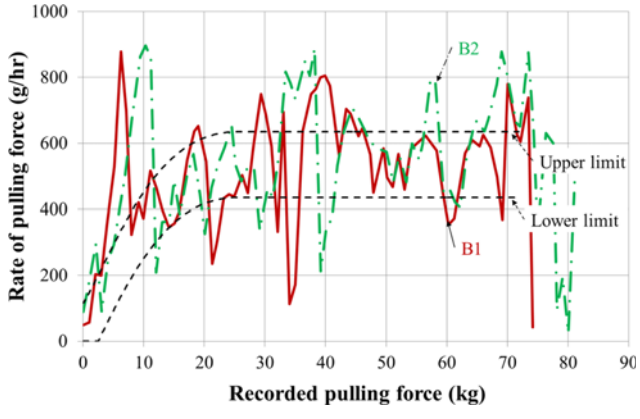


**Fig. 8. The operational control limits of $dF_n/dt$ according to the recorded $F_n$ from B1 and B2 test runs in a 85 kg sapphire grower.**

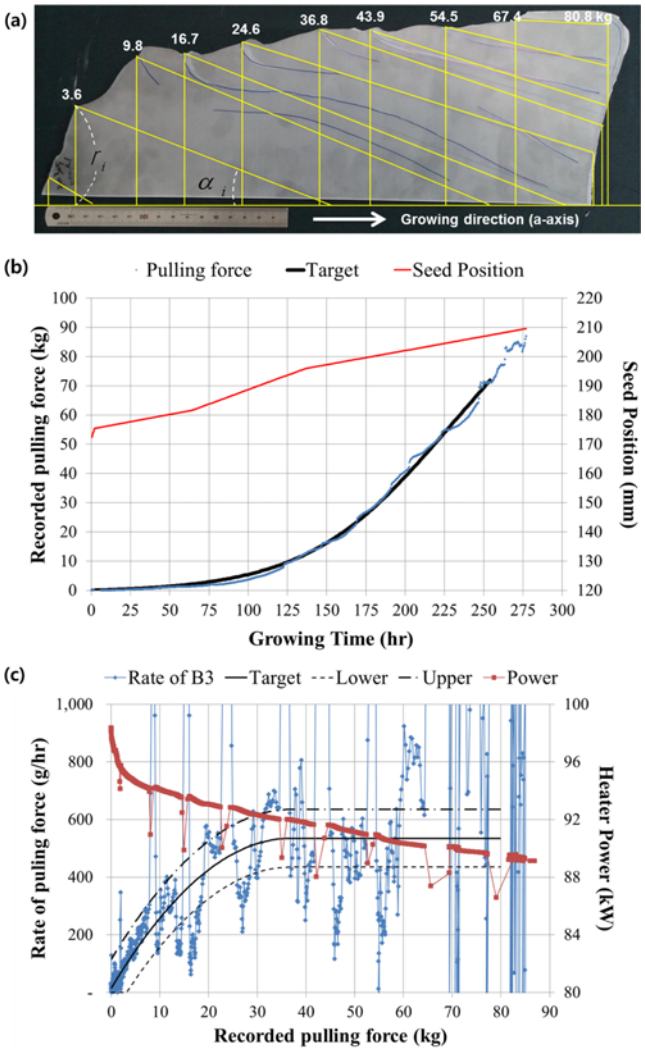


**Fig. 9. The results of comb-pattern experiment in a 85 kg grower (B3). (a) The generated comb-patterns on the vertical slug of B3 boule, (b) the recorded pulling force with the target and seed position profiles and (c) the rate of pulling force with its control limits and heater power profile.**

(3) a stick to a crucible is suspected if the graph shows sudden drop to zero.

In case of (1), the growth rate is overestimated because, when LAGB occurs, the density increases. The oscillation in (2) is due to the change in the buoyancy by the bubbles stuck to the crystal.

In addition, in order to identify the vestige of our conical shape-evolution model, we conducted the comb-pattern experiment with the B3 crystal grown in the 85 kg grower by employing 3-4% power drop for every 25-35 minute duration ((c) in Fig. 9), and at the same time by recording the pulling force and the seed crystal position ((b) in Fig. 9). As shown in Fig. 9(a), the bands of small bubbles appear as the crystal grows along the crystal-melt interface in an axially symmetric mode. Even though the generated bubble streaks are not the exact conical shapes, we can see their propagating trends in the solidification process are enough to be approximated by the conical shape-evolution model.

## CONCLUSIONS

In the current study, the control algorithm for a sapphire single crystal growth is developed based on the mass and the force balances, and is applied to the industrial crystal growth process for the purpose of the crystal quality control of the KY method. First, under the given heat shield, the conical shape-evolution model is theoretically derived from the mass and the energy balances to estimate the apex angle of the con. Then, the control procedure is proposed to increase or decrease the pulling force accordingly. The procedure is validated by applying it to the industrial-scale crystal growth experiments in 85 kg sapphire grower. As a result, the shape and the dynamics of the growing crystal can be estimated. During the crystal growth, small bubbles are generated at the crystal-melt interface and form bands of bubble (so called a comb pattern experiment). Finally, It can be found that the experimental results can also be useful to predict the outbreak of the crystal defect and its type.

## ACKNOWLEDGEMENT

This work was supported by the 2013 Research Fund of the University of Seoul, and the corresponding author gratefully acknowledges it.

## NOMENCLATURE

$C_p$ : heat capacity [J/gK]
F : pulling force [dyn]
g : gravity [980 cm/s$^2$]
h : height of melt [cm]
H : height of crucible [cm]
$\Delta H_s$ : heat of fusion [J/g]
$k_T$ : thermal conductivity [W/mK]
L : length of crystal [cm]
M : mass [g]
n : coordinates normal to a surface [cm]
p : pulling speed [cm/s]
r : radius of crystal [cm]
R : radius of crucible [cm]
S : length from the crystal shoulder to the crystal top [cm]
Ste : Stefan number [-]
T : temperature [K]
$\Delta t$ : time difference [s]
$V_n$ : crystal-melt interface advancing speed [cm/s]

**Greek Letters**

$\alpha$ : halved apex angle on solid-liquid interface [degree]
$\delta$ : characteristic dimensionless number
$\varepsilon$ : tolerance ($=10^{-4}$)
$\Phi$ : function to calculate the volume of cone, truncated cone and cylinder
$\rho$ : density [g/cm$^3$]
$\infty$ : pertaining to bulk

**Subscripts**

0 : initial state at Stage I
B : bottom
c : crystal
i : *i*-th time interval
$l$ : liquid
n : number of time intervals up to time t from $t_0$
T : top

## REFERENCES

1. M. S. Akeselrod and F. J. Bruni, *J. Cryst. Growth*, **360**, 134 (2012).
2. A. Y. Dan'ko, N. S. Sidel'nikova, G. T. Adonkin, A. T. Budnikov, S. V. Nizhankovskii and S. I. Krivonogov, *Crystallography Report*, **49**, 240 (2004).
3. S. D. Vishnevskii, E. V. Krivonosov and L. A. Litvinov, *Crystallography Report*, **53**, 154 (2008).
4. E. R. Dobrovinskaya, L. A. Lytvynov and V. Pishchik, *Sapphire: Material, Manufacturing*, Applications, Springer, Berlin (2009).
5. S. E. Demina, E. N. Bystrova, V. S. Postolov, E. V. Eskov, M. V. Nikolenko, D. A. Marshanin, V. S. Yuferev and V. V. Kalaev, *J. Crystal Growth*, **310**, 1443 (2008).
6. S. E. Demina and V. V. Kalaev, *J. Cryst. Growth*, **320**, 23 (2011).
7. C. H. Chen, J. C. Chen, C. W. Lu and C. M. Liu, *J. Cryst. Growth*, **318**, 162 (2011).
8. C. H. Chen, J. C. Chen, C. W. Lu and C. M. Liu, *J. Cryst. Growth*, **352**, 9 (2012).
9. C. H. Xu, M. F. Zhang, S. H. Meng, J. C. Han, G. G. Wang and H. B. Zuo, *Cryst. Res. Technol.*, **42**, 751 (2007).
10. L. Zhang, H. Zuo, J. Sun, X. Wang, J. Han and D. Xing, *Cryst. Res. Technol.*, **46**, 1019 (2011).
11. L. Zhang, H. Zuo, J. Sun, D. Xing, J. Han and X. Wang, *Cryst. Res. Technol.*, **47**, 175 (2012).
12. Institute for Single Crystal (www.isc.kharkov.com).
13. S. H. Davis, *Theory of solidification*, Cambridge University Press, UK (2001).
14. D. W. Song, E. S. Ji, Y. K. Choi, H. J. Jo and Y. H. Kim, US Patent, 8,349,075 (2013).
15. DK AzTEK (www.dkaztec.com).
16. M. A. Bianchi and R. Viskanta, *Int. J. Heat Mass Transfer*, **40**, 2035

(1997).
17. D. A. Tarzia, *MAT. Series A*, **2**, 1 (2000).

## APPENDIX

This Appendix section will be devoted to address, with an equation-oriented approach, the logical basis of not taking the energy balance into account in the text. To do this, it should be pointed out that (1) temperature in the solid is lower than that of the melt; (2) the axially symmetric geometry is considered; (3) thermal boundary layer formed INSIDE the conical solid surface is likely to be much thinner than its radius of curvature; and (4) heat of fusion, $\Delta H_s$, of $Al_2O_3$ is the only heat source. From these characteristics, it can be readily inferred that heat generated as a result of the solidification is majorly transferred in the direction normal the interface and toward inside of the solid. And the one-dimensional analysis is enough to represent the system.

The equation for the uni-directional (normal to the interface, i.e., n) heat transfer through the solid is

$$\rho C_p \frac{dT}{dt} = k_T \frac{\partial^2 T}{\partial n^2}, \tag{8}$$

which is subjected to the boundary conditions:

$$\rho \Delta H_s V_n = k_T \frac{\partial T}{\partial n} \quad \text{at n=0 (solid-melt interface)}, \tag{9}$$

and

$$T = T_\infty \text{ at } n \to \infty \text{ (thermal boundary layer)}. \tag{10}$$

where $\rho$, $C_p$ and $k_T$ are the density, the heat capacity and the thermal conductivity of $Al_2O_3$, respectively; $V_n$ is the surface advancing speed as a result of the crystal growth, and $T_\infty$ is the bulk temperature in the middle of sapphire crystal.

Eqs. (8) and (9) are rearranged to yield:

$$\frac{dT}{dt} = \frac{k_T}{\rho C_p} \frac{\partial^2 T}{\partial n^2}, \tag{11}$$

and

$$V_n = \frac{k_T}{\rho \Delta H_s} \frac{\partial T}{\partial n}. \tag{12}$$

The group of the constants in Eq. (11) is computed to $8.43 \times 10^{-9}$ $m^2/sK$ and that the group of the constants in Eq. (12), i.e., thermal diusivity, is $1.02 \times 10^{-5}$ $m^2/s$.

It is important to note that the set of equations, Eqs. (11) and (12) subjected to the conditions Eqs. (9) and (10), is a simplified case of the Stefan problem, the closed form solutions of which can be obtained by the method of similarity and found in many literatures [17] and the references therein. The general behaviour of the solution of the Stefan problem depends highly on the dimensionless parameter Ste ($=C_p(T_m - T_\infty)/\Delta H_s$) which is called the Stefan number and measures the ratio of the sensible heat to the latent heat. For the sapphire crystal grow system described in this study, the order of magnitude of Ste is no more than $10^{-2}$, and therefore, the current system is attributed to the small Stefan number problem. It is well-known that, with the small Ste ($10^{-1}$ or less), the Neumann temperature profile becomes linear. Note that the linear profile satisfies the solution of the steady-state problem which means (1) the temperature profile falls into an equilibrium as soon as heat is released as a result of solidification; (2) the crystal growth rate $V_n$ depends majorly on the melt temperature; and (3) the energy balance is not as pivotal as the mass balance in controlling the crystal growth rate. Therefore, the energy balance is possibly ignored during the analysis in this study.